Journal of Biomolecular NMR, **16:** 29–37, 2000.
KLUWER/ESCOM

Intensity modulated HSQC and HMQC: Two simple methods to measure $^3J_{HNH\alpha}$ in proteins

Perttu Permi, Ilkka Kilpeläinen, Arto Annila* & Sami Heikkinen**
Institute of Biotechnology, P.O. Box 56, FIN-00014 University of Helsinki, Helsinki, Finland

Received 20 August 1999; Accepted 22 November 1999

Key words: coupling constants, HB-GAM, HMQC, HSQC, ubiquitin

Abstract

Two methods for the measurement of homonuclear $^3J_{HNH\alpha}$ coupling constants are described. Both HSQC- and HMQC-type experiments employ 'quantitative J-correlation', in which the coupling constant of interest is obtained from the intensity ratio of cross peaks of two spectra. The first spectrum is acquired with $^3J_{HNH\alpha}$ evolution and the second with α-proton decoupling. The resolution of these methods in the F_1-domain is not restricted.

Introduction

The vicinal proton–proton coupling between amide and alpha protons contains important information about protein structure. Already a qualitative inspection of the size of $^3J_{HNH\alpha}$ indicates whether the residue belongs to an α-helix or β-sheet secondary structure. The precise value of the coupling constants can be converted into explicit structural parameters i.e. the Φ-dihedral angle via the Karplus equations (Karplus, 1959; Bystrov, 1976; Vuister and Bax, 1993). There are a number of experimental methods to measure this structurally important coupling constant. Usually, the coupling constant cannot be extracted from 1D protein NMR spectra, due to broad, overlapping resonances. The traditional phase-sensitive COSY experiment (Neuhaus et al., 1985; Ludvigsen et al., 1991; Smith et al., 1991) contains the coupling information in the fine structure of cross peaks between the amide and alpha protons, and the active coupling can be measured from the separation of the antiphase lines. However, in the presence of broad spectral lines the apparent splitting is distorted due to antiphase cancellation and the intensity of the COSY cross peaks will be low as well. Therefore, it is more advantageous to measure the coupling from the in-phase doublet. In the HMQC-J experiment (Forman-Kay et al., 1990; Kay et al., 1990) in-phase cross peaks are split by $^3J_{HNH\alpha}$ in a resolution enhanced F_1-dimension. Recently, we suggested multiplication of the $^3J_{HNH\alpha}$ in the F_1-domain to improve on the resolution (Heikkinen et al., 1999). In addition, a method based on multiple-quantum coherences for the determination of $^3J_{HNH\alpha}$ has been introduced (Rexroth et al., 1995). This method is suitable for double labeled ($^{15}N/^{13}C$) protein samples. It is also possible to utilize E.COSY-type measurements, like HNCA-J (Madsen et al., 1993; Weisemann et al., 1994; Löhr and Rüterjans, 1995), which contain the coupling information in the tilted cross peaks. The HNCA-J experiment also requires double labeled samples, and since high digital resolution in the indirectly detected dimensions is needed, the measurement time of this 3D experiment is long. Possibly the most frequently used methods for measuring $^3J_{HNH\alpha}$ are the so-called 'quantitative J-correlation experiments', where the coupling constant of interest is obtained from the peak intensities. This class of experiments includes the HNHA (Vuister and Bax, 1993; Kuboniwa et al., 1994) and J-modulated HSQC (Billeter et al., 1992) experiments, which do not require double labeled samples. However, these two experiments can be time consuming. This arises from the fact that the HNHA is a 3D experiment and J-modulated HSQC in turn necessitates a series of 2D

*Present address: VTT Chemical Technology, P.O. Box 1401, FIN-02044 VTT, Espoo, Finland.
**To whom correspondence should be addressed. E-mail: tiltu@mimosa.pc.helsinki.fi

experiments. Quite recently, two novel methods, CT-HMQC-HA and CT-HMQC-HN, based on constant time HMQC-J, were described (Ponstingl and Otting, 1998). In these experiments two separate 2D spectra, one with homonuclear $^3J_{HNH\alpha}$ evolution and the other with selective decoupling are recorded. The value for $^3J_{HNH\alpha}$ is measured from the ratio of the cross peak intensities from the two aforementioned spectra. We have worked further on this principle.

Theory

In the CT-HMQC-HA and CT-HMQC-HN experiments (Ponstingl and Otting, 1998) the coupling constant of interest is calculated from the cross peak intensities obtained from two experiments. In the first spectrum the $^3J_{HNH\alpha}$ is allowed to modulate, whereas the second spectrum is recorded in the presence of semi-selective alpha proton decoupling before detection. Equation 1 presents the relation between the experimental $^3J_{HNH\alpha}$ and the two cross peak intensities:

$$I_m/I_d = \cos(\pi^3 J_{HNH\alpha} 2\tau), \quad (1)$$

where I_m and I_d denote the cross peak intensities in the J-modulated and decoupled spectra, respectively. The delay 2τ is the time for the evolution of the $^3J_{HNH\alpha}$. This method is simple, fast, and suitable for samples with ^{15}N-enrichment. In addition, water is easily suppressed. However, the resolution in the F_1-dimension is limited due to the constant-time evolution period. The CT-HMQC-HA experiment inspired us to implement a separate $^3J_{HNH\alpha}$ modulation period into HSQC- and HMQC-experiments. The main advantage of the current method is that the resolution is not restricted by the constant-time evolution period in the F_1-domain.

Description of the pulse sequences

The pulse sequences for the two intensity modulated (IM) experiments, IM-HSQC and IM-HMQC, are presented in Figure 1. The IM-experiments have an additional spin-echo period just after the proton excitation pulse compared with the familiar HSQC/HMQC. During this delay (2τ) the homonuclear coupling $^3J_{HNH\alpha}$ is active for the coupled experiment, and it is effectively decoupled during 2τ in the decoupled experiment. After the delay 2τ, which also includes the polarization transfer delay 2Δ, the IM-HSQC continues as the conventional HSQC. In the IM-HMQC sequence, the alpha proton is decoupled after the delay 2τ for both experiments. This ensures that the homonuclear $^3J_{HNH\alpha}$ coupling is not active during other delays than 2τ. The semi-selective alpha proton decoupling in IM-HSQC and IM-HMQC was performed by applying the off-resonance G3-cascade (Emsley and Bodenhausen, 1990) to the alpha proton region. Alternatively, two semi-selective inversion pulses in the middle of the τ periods can be used to decouple the alpha protons. The water signal was suppressed in all pulse sequences by the WET sequence (Smallcombe et al., 1995) prior to the excitation pulse.

The product operator analysis (Sørensen et al., 1983) for IM-HSQC was performed for the H^NNH^α spin system considering only the delay period 2τ, which also contains the INEPT-transfer delay 2Δ.

(A) Coupled experiment:

$$H_Z^N H_I^A N_I \xrightarrow{90^\circ_x(H)} -H_Y^N H_I^A N_I \xrightarrow{\tau - 180^\circ_x(H) - (\tau-\Delta) - 180^\circ_x(N) - \Delta}$$
$$H_Y^N H_I^A N_I \cos(\pi^3 J_{HNH\alpha} 2\tau) \cos(\pi^1 J_{HN} 2\Delta)$$
$$-H_X^N H_Z^\alpha N_I \sin(\pi^3 J_{HNH\alpha} 2\tau) \cos(\pi^1 J_{HN} 2\Delta)$$
$$-H_X^N H_I^\alpha N_Z \cos(\pi^3 J_{HNH\alpha} 2\tau) \sin(\pi^1 J_{HN} 2\Delta)$$
$$-H_Y^N H_Z^\alpha N_Z \sin(\pi^3 J_{HNH\alpha} 2\tau) \sin(\pi^1 J_{HN} 2\Delta)$$

(B) Decoupled experiment:

$$H_Z^N H_I^\alpha N_I \xrightarrow{90^\circ_x(H)} -H_Y^N H_I^\alpha N_I \xrightarrow{\tau - 180^\circ_x(H) - (\tau-\Delta) - 180^\circ_x(N) - \Delta}$$
$$H_Y^N H_I^\alpha N_I \cos(\pi^1 J_{HN} 2\Delta)$$
$$-H_X^N H_I^\alpha N_Z \sin(\pi^1 J_{HN} 2\Delta)$$

Only the terms of type $H_X^N H_I^\alpha N_Z$ will be converted into heteronuclear single-quantum coherence by the simultaneous 90° pulses on proton and nitrogen of the INEPT element and thus ultimately contribute the detected magnetization. It should be pointed out that any additional free precession delays, for example during gradients, allow the evolution of the proton chemical shifts of type $H_Y^N H_X^\alpha N_Y$ (originating from operator $H_Y^N H_Z^\alpha N_Z$ in the coupled experiment), which is a superposition of heteronuclear triple- and single-quantum coherences. This term would then give rise to observable magnetization in the coupled experiment, which in turn would distort the cross-peak intensities of the coupled IM-HSQC spectrum. Hence, addition of the sensitivity-enhancement scheme (Kay et al., 1992) in the pulse sequence is not easily accomplished. However, this could be done by utilizing alpha proton decoupling during the reverse-INEPT steps.

The product operator analysis for the IM-HMQC experiment considering only the delay 2τ is as follows:

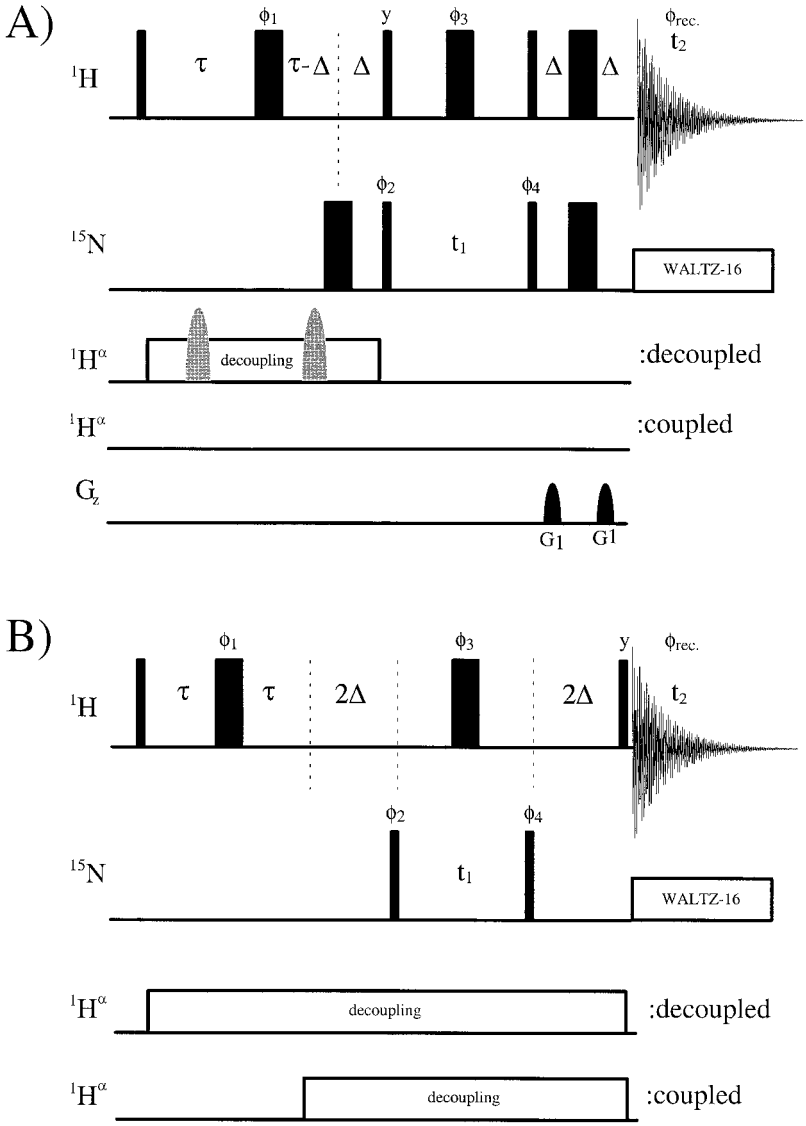

Figure 1. IM-HSQC (A) and IM-HMQC (B) pulse sequences for measuring $^3J_{HNH\alpha}$ coupling constants. Hard 90° and 180° pulses are indicated by narrow and wide bars, respectively. All pulses are applied with phase x unless indicated otherwise. Delay durations: $\Delta = 1/4J_{HN}$, $2\tau < 1/2^3J_{HNH\alpha max}$. (A) IM-HSQC. Phase cycling: ϕ_1 = x,x,y,y,−x,−x,−y,−y; ϕ_2 = x,−x; ϕ_3 = x; ϕ_4 = 8(x),8(−x); ϕ_{rec} = 2(x,−x,−x,x),2(−x,x,x,−x). Phase ϕ_2 is incremented in the States-TPPI manner (Marion et al., 1989). Gradient strength (duration) G_1: 7.2 G/cm (0.5 ms). Gradient recovery time = 200 μs. (B) IM-HMQC. Phase cycling: ϕ_1 = x,x,y,y,−x,−x,−y,−y; ϕ_2 = x,−x; ϕ_3 = 16(x),16(−x); ϕ_4 = 8(x),8(−x); ϕ_{rec} = 2(x,−x,−x,x),2(−x,x,x,−x). Phase ϕ_2 is incremented in the States-TPPI manner. Two spectra for each experiment are collected, with and without alpha proton decoupling during 2τ. These two data sets are referred to as 'decoupled' (I_d) and 'coupled' (I_m). Semi-selective alpha proton decoupling during the J-modulation delay, 2τ, was achieved either by applying a G3 pulse cascade or two REBURP pulses to the alpha proton region (3–5 ppm). The WET solvent suppression scheme is applied onto the water resonance prior to the actual experiments. Gradient strengths (durations) for the WET sequence: g_1 = 32 (2 ms), g_2 = 18.1 (2 ms), g_3 = 7.9 (2 ms), g_4 = 4.1 (2 ms) G/cm. Decoupling of ^{15}N during the acquisition was performed using the WALTZ-16 sequence (Shaka et al., 1983).

(A) Coupled experiment:

$$H_Z^N H_I^\alpha N_I \xrightarrow{90^\circ_x(H)} -H_Y^N H_I^\alpha N_I \xrightarrow{\tau - 180^\circ_x(H) - \tau}$$
$$H_Y^N H_I^\alpha N_I \cos(\pi {}^3J_{HNH\alpha} 2t) - H_X^N H_Z^\alpha N_I \sin(\pi {}^3J_{HNH\alpha} 2\tau)$$

(B) Decoupled experiment:

$$H_Z^N H_I^\alpha N_I \xrightarrow{90^\circ_x(H)} -H_Y^N H_I^\alpha N_I$$
$$\xrightarrow{\tau - 180^\circ_x(H) - \tau} H_Y^N H_I^\alpha N_I$$

The purging 90° pulse on protons with y-phase just before acquisition in the IM-HMQC sequence is not necessary, as the $H_X^N H_Z^\alpha N_I$ magnetization, which is formed in the coupled experiment during the delay 2τ, is effectively destroyed by the alpha proton decoupling starting at the beginning of the delay 2Δ.

After measuring the cross peak intensities of the decoupled and coupled spectra, the coupling constant for both the IM-HSQC and IM-HMQC experiments can be calculated from Equation 1.

Results and discussion

The presented methods rely solely on the cross peak intensity difference in two separate experiments. Therefore any undesired phenomena that differently affect the signal intensity between the two experiments must be minimized or corrected. Relaxation will have significant impact on the measured J-coupling if the relaxation rate approaches the size of the coupling constant of interest (Harbison, 1993). In case of rapid spin flips of the alpha proton, the measured $^3J_{HNH\alpha}$ gives an underestimate of the true $^3J_{HNH\alpha}$ since in the decoupled experiment the intensity is reduced due to different relaxation properties of the in- and antiphase magnetization of the amide proton with respect to the alpha proton. The spin-flip rate is nearly linearly proportional to the isotropic rotational correlation time τ_c of the protein (Vuister and Bax, 1993; Kuboniva et al. 1994; Ponstingl and Otting, 1998). A correction coefficient for a particular experiment can be calculated if τ_c is known.

Attention should also be paid to the frequency selectivity of the alpha proton decoupling. On the one hand, decoupling or inversion performance should be proper and uniform within the selected region. In addition, the semi-selective decoupling must not affect the amide proton region. This could be investigated by varying the bandwidth or offset of the decoupling pulses and monitoring the intensity of the amide proton signals.

Table 1. Comparison of measured $^3J_{HNH\alpha}$ coupling constants for some residues of human ubiquitin from IM-HSQC, IM-HMQC and CT-HMQC-HA experiments

Residue	IM-HSQC	IM-HMQC	CT-HMQC-HA	Karplus
Ile3	8.9	8.2	8.4	9.6
Val5	9.9	9.0	9.7	9.9
Lys11	6.1	5.4	6.6	8.7
Ile13	9.4	9.7	9.5	9.6
Leu15	9.4	9.6	9.6	9.8
Glu18	9.3	9.5	9.4	9.9
Asn25	4.4	4.2	4.9	4.8
Lys27	4.3	4.1	–	4.2
Lys29	4.2	4.3	4.4	4.7
Ile30	4.3	5.5	5.1	5.4
Asp32	2.3	3.1	3.4	3.3
Lys33	6.5	6.6	6.5	8.4
Ile36	6.2	5.3	5.5	6.7
Gln40	9.1	9.1	9.0	8.6
Leu50	6.7	6.7	6.6	6.7
Arg54	8.9	8.4	9.3	7.5
Asp58	4.5	4.3	3.0	3.6
Tyr59	8.4	8.6	8.7	8.1
Asn60	7.0	7.2	6.9	6.3
Ile61	6.5	7.2	6.3	7.9
His68	9.4	9.7	9.6	9.4

All the spectra were recorded using the same delay for $^3J_{HNH\alpha}$ evolution (the delay 2τ was set to 40 ms for IM-HSQC and IM-HMQC, and the total length of the CT-HMQC-HA sequence was also set to 40 ms). The experimental J-coupling constants were determined from IM-HSQC, IM-HMQC and CT-HMQC-HA spectra as mentioned in the text. J-coupling values from the X-ray structure were calculated using the Karplus relationship (Vuister and Bax, 1993). The residues Asn25, Lys27, Lys29, Ile30, Asp32, Lys33, Asp58, and Tyr59 are situated in an α-helical region, which is in concordance with experimental coupling constants.

Furthermore, possible random instabilities in spectrometer performance may lead to errors in the cross peak intensities. Therefore, it is beneficial to accumulate with a maximum number of transients, while maintaining the desired resolution in F_1, with respect to the available measurement time in order to minimize these errors.

The IM-HSQC and IM-HMQC pulse sequences were tested with a ^{15}N-labeled human ubiquitin sample (76 residues, 8.6 kDa). The results were compared to those obtained from the CT-HMQC-HA, and with values derived from the crystal structure. An identical decoupling scheme, the off-resonance G3-cascade (Emsley and Bodenhausen, 1990), was used for both the IM-HSQC/IM-HMQC and the CT-HMQC-HA

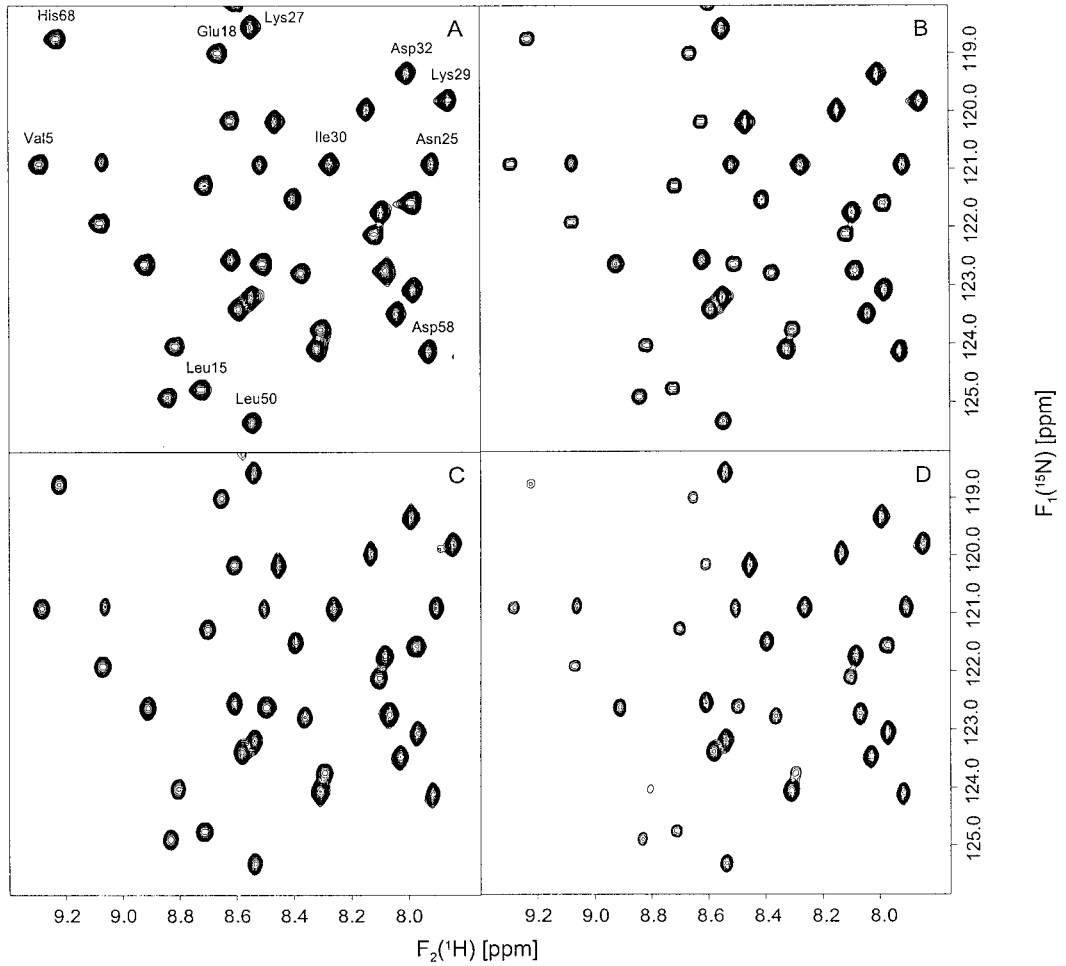

Figure 2. Representative expansion of IM-HSQC and IM-HMQC spectra of ubiquitin recorded on a Varian Unity 500 spectrometer (500 MHz proton frequency) equipped with a triple resonance probe ($^{1}H/^{15}N/^{13}C$) and z-axis self-shielded gradient system. IM-HSQC: the decoupled spectrum (A) was obtained by applying semi-selective alpha proton decoupling during delay 2τ; (B) represents the coupled spectrum from the same spectral region. IM-HMQC: decoupled (C) and coupled (D) spectra from the same spectral region as for the spectra presented in (A) and (B). Sample conditions: 1 mM ^{15}N-enriched human ubiquitin from VLI Research Inc. in 90%/10% H_2O/D_2O, pH 5.8, 50 mM sodium phosphate buffer, 30 °C. Spectral widths in the F_1- (F_2-) dimension = 1700 (8000) Hz, number of t_1 increments = 200, number of transients = 64, acquisition time (t_2) = 128 ms. Data were zero-filled to 1K in the F_1-dimension, a squared cosine window function was applied in the F_1- and F_2-dimensions. Processing was performed using the Felix 97.0 software package (Biosym/MSI, 1997).

experiment to ensure that the possible decoupling-induced distortions in the intensities are identical for every experiment, thus enabling direct comparison between the experiments. Table 1 contains the representative results for ubiquitin. The results from the CT-HMQC-HA, IM-HSQC, and IM-HMQC spectra are not corrected for the relaxation effects as the experiments were performed just for evaluation purposes. As can be seen from Table 1, the results obtained with these three different methods are in good agreement. We estimate that the presented methods are capable of producing $^{3}J_{HNH\alpha}$ values with a precision of ca. 0.5–1.0 Hz, indicating that the precision is sufficient for practical purposes. Considering coupling constants of 4–5 Hz, typical for residues in α-helical regions, the experimental inaccuracy is larger than for the couplings (8–11 Hz) found in β-sheet structures due to the nature of the experiment. On the other hand, according to the Karplus equation, the significance of the experimental error is smaller for α-helical values than for β-sheet values. This is due to the relatively narrow Φ-range (∼20°) corresponding to $^{3}J_{HNH\alpha}$-values (∼4–6 Hz) found in α-helical substructures.

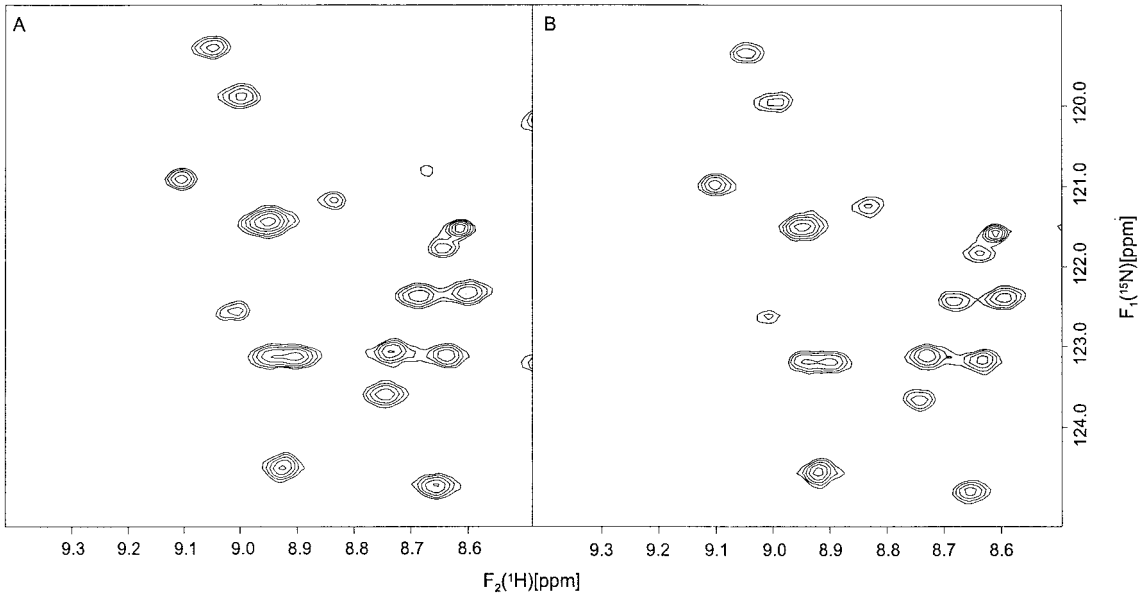

Figure 3. Representative expansion of IM-HSQC spectra of HB-GAM recorded on a Varian Unity 500 spectrometer (500 MHz proton frequency) equipped with a triple resonance probe ($^{1}H/^{15}N/^{13}C$) and z-axis self-shielded gradient system. IM-HSQC: the decoupled spectrum (A) was obtained by applying an alpha proton semi-selective REBURP pulse during each τ delay; (B) represents the coupled spectrum from the same spectral region. Sample conditions: 1.1 mM ^{15}N-enriched HB-GAM in 95%/5% H_2O/D_2O, pH 4.7, 30 °C. Spectral widths in the F_1-(F_2-) dimension = 1700 (8000) Hz, number of t_1 increments = 240, number of transients = 64, acquisition time (t_2) = 128 ms. Data were zero-filled to 1K in the F_1-dimension, a squared cosine window function was applied in the F_1- and F_2-dimensions. Processing was performed using the Felix 97.0 software package (Biosym/MSI, 1997).

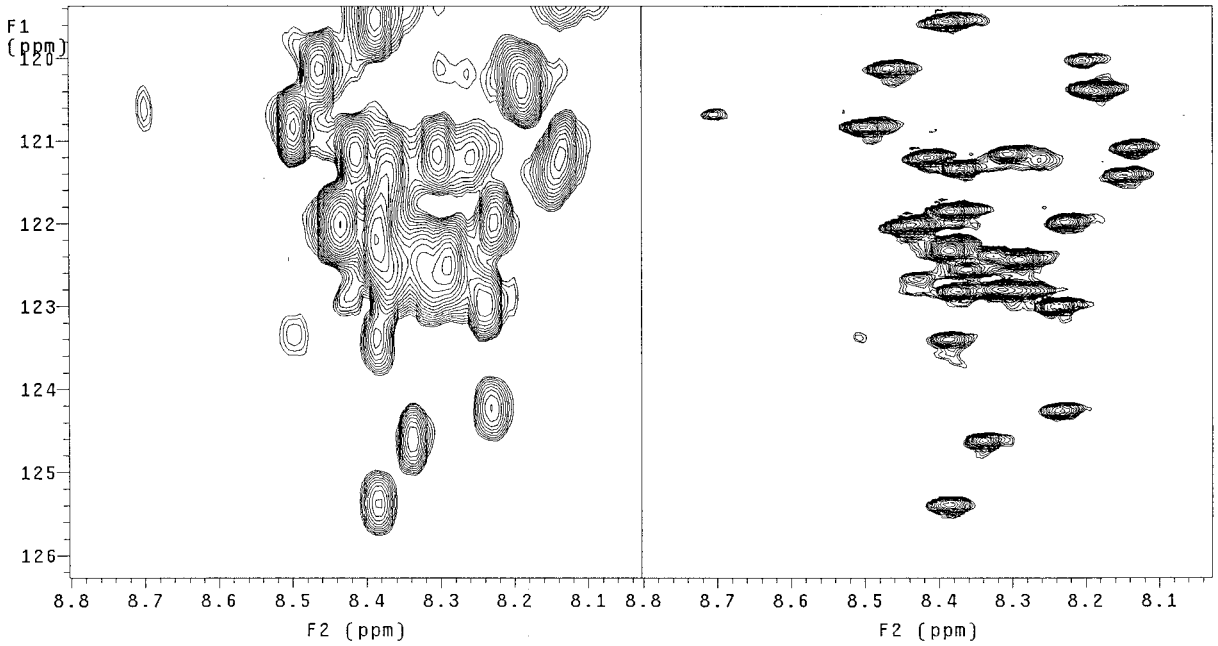

Figure 4. Representative expansion of coupled CT-HMQC-HA (left) and IM-HSQC (right) spectra of HB-GAM recorded on a Varian Inova 500 spectrometer (500 MHz proton frequency) equipped with a triple resonance probe ($^{1}H/^{15}N/^{13}C$) and z-axis self-shielded gradient system. Experimental parameters were the same as in Figure 3 except for (CT-HMQC-HA) number of t_1 increments = 50, number of transients = 32; (IM-HSQC) number of t_1 increments = 240, number of transients = 32. Data were zero-filled to 2K (4K) in the F_1-dimension (F2-dimension), a cosine window function was applied in the F_1- and F_2-dimensions. Processing was performed using the Vnmr 6.1 software package (Varian Associates, 1998).

Figures 2A and 2B show representative expansions of the decoupled and coupled IM-HSQC spectra of ubiquitin, respectively. The same regions of the decoupled and coupled IM-HMQC spectra are shown in Figures 2C and 2D. For the determination of $^3J_{HNH\alpha}$ coupling constants, the cross peak volumes for the decoupled and coupled experiments were measured using identical integration regions.

The measured coupling constant values (uncorrected with respect to relaxation effects) from the IM-HSQC and IM-HMQC methods are in good agreement with the results obtained utilizing the established CT-HMQC-HA method, as well as with the $^3J_{HNH\alpha}$ values calculated via Karplus equations from the crystal structure of ubiquitin (Vijay-Kumar et al., 1987). The $^3J_{HNH\alpha}$ for residue Lys27 could not be measured using CT-HMQC-HA due to cross peak overlap resulting from the limited resolution in the F_1-domain ($t_{1max} = 28.2$ ms). This could be avoided by increasing the modulation time, allowing more t_1-increments in the F_1-dimension. However, for large homonuclear couplings, nulling of the cross peak intensities should be avoided (e.g. $2\tau = 50$ ms results in null-intensity for residues with $^3J_{HNH\alpha} = 10$ Hz). A possible reason for deviations from 'Karplus' values for Lys11 and Lys33 may originate either from differences between crystal and liquid state structures or from possible inappropriate excitation of either the amide or alpha protons by G3-cascade. The latter could be tested by further experiments using a different offset and/or bandwidth for decoupling.

The pulse sequence utilizing two selective pulses for homonuclear decoupling (Figure 1A) was applied for the measurement of $^3J_{HNH\alpha}$ values from heparin binding growth associated molecule, HB-GAM (15 kDa, 136 amino acid residues) (Rauvala et al., 1994; Peng et al., 1995; Rauvala and Peng, 1997; Kilpeläinen et al., 2000). HB-GAM is an extracellular matrix-associated protein implicated in the development and plasticity of neuronal connections in the brain.

Figure 3 shows representative regions of IM-HSQC spectra of HB-GAM. The effects of different relaxation rates of in- and antiphase magnetizations on cross peak intensities for coupled and decoupled experiments were calculated using an analogous procedure to the one described by Ponstingl and Otting (1998). A J-modulation period of 30 ms and a spin-flip rate of 9.75 Hz were used to calculate the effects of relaxation. According to these calculations, the experimental values of $^3J_{HNH\alpha}$ of HB-GAM are approximately 6% too small. Therefore, an overall correction coefficient of 1.06 can be estimated for $^3J_{HNH\alpha}$'s of HB-GAM measured using this particular experiment. The gain in resolution is clearly demonstrated in Figure 4, presenting expansions of coupled CT-HMQC-HA and IM-HSQC spectra of HB-GAM. Experiment times were 4 h 51 min and 51 min, respectively. Although the sensitivity of IM-HSQC is lower, the achievable resolution allows more $^3J_{HNH\alpha}$'s to be measured, thus it is obvious that the loss of sensitivity is acceptable for improved resolution.

The selective REBURP inversion/refocusing pulse was chosen for alpha proton decoupling due to its good excitation profile (Geen and Freeman, 1991). To correct the effects of relaxation, the alpha proton spin-flip rate was estimated from the rotational correlation time τ_c of HB-GAM using the known τ_c's and spin-flip rates of human ubiquitin (Cavanagh et al., 1996) and staphylococcal nuclease, SNase (Vuister and Bax, 1993). The correlation time τ_c, 7.8 ns, of HB-GAM was obtained from ^{15}N T_1- and T_2-measurements (Farrow et al., 1994).

Table 2 lists 17 $^3J_{HNH\alpha}$ coupling constant values (uncorrected and corrected) of HB-GAM. The total number of measurable coupling constants was more than 100, 61 of which were used in structure calculations. The measured coupling constants are in good agreement with the secondary structure of HB-GAM (Kilpeläinen et al., 2000).

As the IM-HSQC and IM-HMQC methods rely on the intensity comparison of two cross peaks in two separate spectra, the delay 2τ should be adjusted such that the difference between the two intensities is large. However, the delay 2τ cannot be equal to $1/2(^3J_{HNH\alpha})$, as this condition results in nulling of the intensity. Also the relaxation of the amide protons will limit the delay length. In practice, it is advisable to record decoupled and the coupled spectra with two different 2τ delay lengths, for instance with 20 ms and 40 ms, favourable for large and small coupling constants, respectively.

As the IM-HMQC sequence contains less 180° pulses, it could be less sensitive to offset- and pulse miscalibration effects. On the other hand, water suppression can be more easily constructed within the HSQC-based sequence. Furthermore, the need for alpha proton decoupling during the incremented delay can be avoided with IM-HSQC.

Table 2. $^3J_{HNH\alpha}$ values for residues 96–112 of HB-GAM

Residue	$^3J_{HNH\alpha}$	$^3J_{HNH\alpha}$
	Not corrected	Corrected
Asn96	7.3	7.7
Ala97	1.3	1.4
Asp98	7.3	7.7
Cys99	1.0	1.1
Gln100	3.9	4.1
Lys101	1.6	1.7
Thr102	7.6	8.1
Val103	9.0	9.5
Thr104	8.5	9.0
Ile105	10.6	11.2
Ser106	1.7	1.8
Lys107	8.3	8.8
Pro108	–	–
Cys109	6.6	7.0
Gly110	–	–
Lys111	6.9	7.3
Leu112	7.1	7.5

Proline does not have an amide proton and the method is not suitable for glycines (for P108 and G110, no $^3J_{HNH\alpha}$ value is given in the table). Both uncorrected and corrected values, with respect to relaxation, are presented. The data were recorded using the pulse sequence presented in Figure 1A. Homonuclear decoupling during the J-modulation delay was achieved by applying two semi-selective REBURP pulses to the alpha proton region. The length of the J-modulation delay, 2τ, was set to 30 ms. The spin-flip rate of HB-GAM (9.75 Hz) and this particular experimental set-up results in a correction coefficient of magnitude 1.06.

Conclusions

In conclusion, we have demonstrated two methods for the measurement of $^3J_{HNH\alpha}$ coupling constants in the polypeptide backbone. These methods allow accurate, simple and rapid measurement of $^3J_{HNH\alpha}$ coupling constants. The spectral resolution in the F_1-domain of these methods is not restricted by a constant time, thus the resolution can be set independently of the delay used for J-modulation. This can be essential in the case of larger proteins with more crowded spectra. On the other hand, the CT-HMQC-HA takes advantage of slower relaxation of ^1H-^{15}N multiple-quantum coherence compared to amide proton single-quantum coherence. This can be of some importance with larger proteins. The presented method can be modified into such a form that the homonuclear J-modulation takes place in the presence of ^1H-^{15}N multiple-quantum coherence prior to the ^{15}N chemical shift evolution, thus enabling unrestricted resolution.

Acknowledgements

This work was supported by the Academy of Finland. Hanna Avikainen is acknowledged for supplying us the T_1- and T_2-data of HB-GAM. We are grateful to Tarja Kinnunen for preparation of the HB-GAM sample.

References

Billeter, M., Neri, D., Otting, G., Qian, Y.Q. and Wüthrich, K. (1992) *J. Biomol. NMR*, **2**, 257–274.
Bystrov, V.F. (1976) *Progr. NMR Spectrosc.*, **10**, 41–81.
Cavanagh, J., Fairbrother, W.J., Palmer, A.G. and Skelton, N.J. (1996) *Protein NMR Spectroscopy: Principles and Practice*, Academic Press, San Diego, CA.
Emsley, L. and Bodenhausen, G. (1990) *Chem. Phys. Lett.*, **165**, 469–476.
Farrow, N., Muhandiram, D.R., Singer, A.U., Pascal, S.M., Kay, C.M., Gish, G., Shoelson, S.E., Pawson, T., Forman-Kay, J.D. and Kay, L.E. (1994) *Biochemistry*, **33**, 5984–6003.
FELIX 97.0 (1997), Biosym/MSI, San Diego, CA.
Forman-Kay, J.D., Gronenborn, A.M., Kay, L.E., Wingfield, P.T. and Clore, M. (1990) *Biochemistry*, **29**, 1566–1572.
Geen, H. and Freeman, R. (1991) *J. Magn. Reson.*, **93**, 93–141.
Harbison, G. (1993) *J. Am. Chem. Soc.*, **115**, 3026–3027.
Heikkinen, S., Aitio, H., Permi, P., Folmer, R., Lappalainen, K. and Kilpeläinen, I. (1999) *J. Magn. Reson.*, **137**, 243–246.
Karplus, M. (1959) *J. Chem. Phys.*, **30**, 11–15.
Kay, L.E. and Bax, A. (1990) *J. Magn. Reson.*, **86**, 110–126.
Kay, L.E., Keifer, P. and Saarinen, T. (1992) *J. Am. Chem. Soc.*, **114**, 10663–10665.
Kilpeläinen, I., Kaksonen, M., Kinnunen, T., Raulo, E., Avikainen, H., Fath, M., Linhardt, R.J., and Rauvala, H. (2000) *J. Biol. Chem.*, accepted for publication.
Kuboniwa, H., Grzesiek, S., Delaglio, F. and Bax, A. (1994) *J. Biomol. NMR*, **4**, 871–878.
Löhr, F. and Rüterjans, H. (1995) *J. Biomol. NMR*, **5**, 25–36.
Ludvigsen, S., Andersen, K.V. and Poulsen, F.M. (1991) *J. Mol. Biol.*, **217**, 731–736.
Madsen, J.C., Sørensen, O.W., Sørensen, P. and Poulsen, F.M. (1993) *J. Biomol. NMR*, **3**, 239–244.
Marion, D., Ikura, M., Tschudin, R. and Bax, A. (1989) *J. Magn. Reson.*, **85**, 393–399.
Neuhaus, D., Wagner, G., Vasak, M., Kägi, J.H.R. and Wüthrich, K. (1985) *Eur. J. Biochem.*, **151**, 257–273.
Peng, H.B., Ali, A.A., Dai, Z., Dagget, D.F., Raulo, E. and Rauvala, H. (1995) *J. Neurosci.*, **15**, 3027–3038.
Ponstingl, H. and Otting, G. (1998) *J. Biomol. NMR*, **12**, 319–324.
Rauvala, E., Vanhala, A., Castren, E., Nolo, R., Raulo, E., Merenmies, J. and Panula, P. (1994) *Dev. Brain Res.*, **79**, 157–176.
Rauvala, H. and Peng, P. (1997) *Progr. Neurobiol.*, **52**, 127–144.

Rexroth, A., Schmidt, P., Szalma, S., Geppert, T., Schwalbe, H. and Griesinger, C. (1995) *J. Am. Chem. Soc.*, **113**, 10389–10390.

Shaka, A.J., Keeler, J., Frenkiel, T. and Freeman, R. (1983) *J. Magn. Reson.*, **52**, 334–338.

Smallcombe, S.H., Patt, S.L. and Keifer, P.A. (1995) *J. Magn. Reson.*, **A117**, 295–303.

Smith, L.J., Sutcliffe, M.J., Redfield, C. and Dobson, C.M. (1991) *Biochemistry*, **30**, 986–996.

Sørensen, O.W., Eich, G.W., Levitt, M.H., Bodenhausen, G. and Ernst, R.R. (1983) *Progr. NMR Spectrosc.*, **16**, 163–192.

Vijay-Kumar, S., Bugg, C.E. and Cook, W.J. (1987) *J. Mol. Biol.*, **194**, 531–544.

Vuister, G.W. and Bax, A. (1993) *J. Am. Chem. Soc.*, **115**, 7772–7777.

Weisemann, R., Rüterjans, H., Schwalbe, H., Schleucher, J., Bermel, W. and Griesinger, C. (1994) *J. Biomol. NMR*, **4**, 231–240.